

A ROTATING MOLECULAR JET FROM A PERSEUS PROTOSTAR

GERARDO PECH, LUIS A. ZAPATA, LAURENT LOINARD*, AND LUIS F. RODRÍGUEZ

Centro de Radioastronomía y Astrofísica, Universidad Nacional Autónoma de México, Morelia 58090, Mexico

To appear in ApJ

ABSTRACT

We present ¹²CO(2-1) line and 1.4 mm continuum archival observations, made with the Submillimeter Array, of the outflow HH 797 located in the IC 348 cluster in Perseus. The continuum emission is associated with a circumstellar disk surrounding the class 0 object IC 348-MMS/SMM2, a very young solar analog. The line emission, on the other hand, delineates a collimated outflow, and reveals velocity asymmetries about the flow axis over the entire length of the flow. The amplitude of velocity differences is of order 2 km s⁻¹ over distances of about 1000 AU, and we interpret them as evidence for jet rotation —although we also discuss alternative possibilities. A comparison with theoretical models suggests that the magnetic field lines threading the protostellar jet might be anchored to the disk of a radius of about 20 AU.

Subject headings: stars: formation — ISM: jets and outflows — ISM: individual objects (IC348)

1. INTRODUCTION

Molecular outflows are one of the first manifestations of the formation of a new star. They are thought to play an essential role in the removal of angular momentum from collapsing dense cores, which eventually enable them to contract to stellar sizes. Although the details remain unclear, the general consensus is that outflows are driven by rotating magnetic fields anchored to the disk-star system (Pudritz et al. 2007; Shang et al. 2007). Accretion disks are known to rotate, so the material ejected from them should inherit a toroidal angular momentum component (Fendt 2011). Indeed, observational evidence for this component have been presented for several outflows driven by young stellar objects (Choi et al. 2011; Zapata et al. 2010; Launhardt et al. 2009; Lee et al. 2009, 2008).

Arguably the most direct evidence has been presented by Launhardt et al. (2009) who reported millimeter interferometric observations of the isolated Bok globule CB 26. Their ¹²CO(2-1) line observations revealed the presence of a systematic velocity gradient perpendicular to the flow axis along its entire length. Zapata et al (2010), on the other hand, reported three independent ¹²CO(2-1) and SO(6-5) observations toward the Ori-S6 molecular outflow. All three observations revealed velocity asymmetries about the outflow axis which are suggestive of rotation at different size scales.

IC 348 is a young star cluster (~ 2 Myr) located near the eastern edge of the Perseus dark cloud complex at about 300 pc from the sun (Muench et al. 2007; Luhman et al. 2003). It contains more than a dozen protostars, many of them driving outflows. The IC 348-MMS/SMM2 source is a dense condensation within that region which drives a large collimated north-south CO outflow (Tafalla et al. 2006; Hatchell & Dunham 2009). The optical and infrared counterpart of this molecular outflow is the Herbig-Haro system HH 797 (McCaughrean et al. 1994; Eisloffel et al. 2003; Walawender et al. 2005, 2006). The low radial ve-

locities displayed by the outflow (blue to the north and red to the south) and its large extension (~ 0.5 pc) suggest that it is nearly in the plane of the sky.

In this study, we present millimeter observations, made with the Submillimeter Array¹ (SMA), of the IC 348-MMS/SMM2 object and its associated HH 797 outflow. These interferometric observations reveal velocity asymmetries about the flow axis over the entire length of the flow, that will be interpreted as jet rotation.

2. OBSERVATIONS

The observations were obtained from the SMA archive, and were collected on November 2005, when the array was in its compact configuration. The 21 independent baselines in the compact configuration ranged in projected length from 10 to 55 k λ . The phase reference center for the observations was at $\alpha_{J2000.0} = 03^{\text{h}}43^{\text{m}}57^{\text{s}}.29$, $\delta_{J2000.0} = +32^{\circ}03'09''.0$. Two frequency bands, centered at 220.538 GHz (Lower Sideband) and 230.538 GHz (Upper Sideband) were observed simultaneously. The observations were made in mosaicing mode using the half-power point spacing between field centers and thus covering the entire HH 797 outflow. The primary beam of the SMA at 230 GHz has a FWHM $\sim 50''$.

The SMA digital correlator was configured in 24 spectral windows (“chunks”) of 104 MHz and 128 channels each. This provides a spectral resolution of 0.812 MHz (~ 1.1 km s⁻¹) per channel. The zenith opacity ($\tau_{230\text{GHz}}$), measured with the NRAO tipping radiometer located at the nearby Caltech Submillimeter Observatory, fluctuated between 0.12 and 0.19, indicating reasonable weather conditions during the observations. Observations of Uranus provided the absolute scale for the flux density calibration. The gain calibrators were the quasars 3C 111 and 3C 84, while 3C 273 was used for bandpass calibration. The uncertainty in the flux scale is estimated to be between 15 and 20%, based on the SMA monitoring of quasars. Further technical descriptions of

¹ The Submillimeter Array (SMA) is a joint project between the Smithsonian Astrophysical Observatory and the Academia Sinica Institute of Astronomy and Astrophysics, and is funded by the Smithsonian Institution and the Academia Sinica.

*Max-Planck-Institut für Radioastronomie, Auf dem Hügel 69 53121 Bonn, Alemania

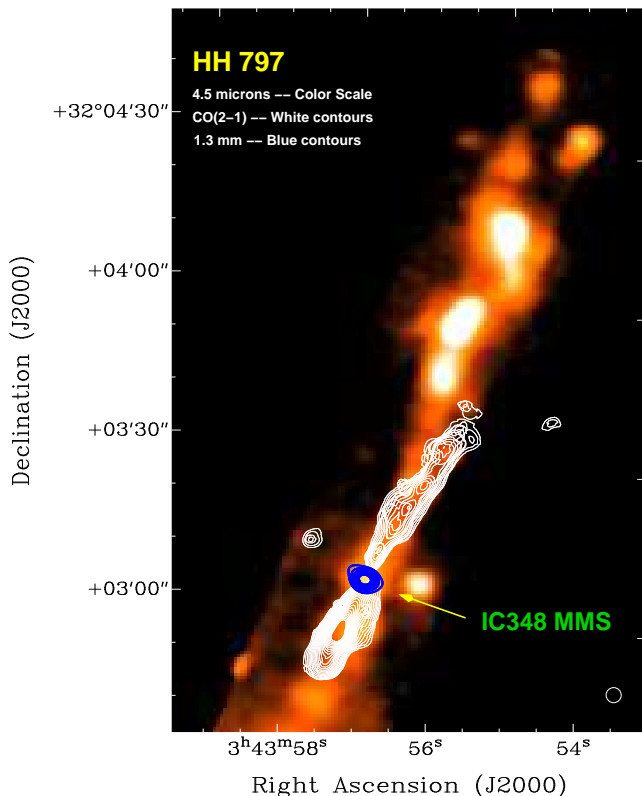


FIG. 1.— SMA CO(2-1) integrated intensity map (moment 0) of HH 797 (white contours) overlaid with a $4.5 \mu\text{m}$ Spitzer-IRAC image (color scale), and the 1.4 mm continuum emission from the object IC 348-MMS/SMM2 (blue contours). The white contours range from 15% to 80% of the emission peak in steps of 5%. The emission peak for the CO(2-1) observations is $31 \text{ Jy beam}^{-1} \text{ km s}^{-1}$. The blue contours range from 40% to 90% of the peak emission in steps of 9%. The emission peak for the millimeter continuum observations is $160 \text{ mJy beam}^{-1}$. The synthesized beam of the line and continuum observations is shown in the lower right corner.

the SMA and its calibration schemes can be found in Ho et al. (2004).

The data were calibrated using the IDL superset MIR, originally developed for the Owens Valley Radio Observatory (OVRO, Scoville et al. 1993) and adapted for the SMA.² The calibrated data were imaged and analyzed in the standard manner using the MIRIAD and KARMA (Gooch 1996) softwares. A 1.4 mm continuum image was obtained by averaging line-free channels in the upper sideband. We set the ROBUST parameter of the task INVERT to 0 to obtain an optimal compromise between resolution and sensitivity. The resulting r.m.s. noise for the continuum image was about 7 mJy beam^{-1} at an angular resolution of $3''.42 \times 3''.20$ with a P.A. = -70.8° . The r.m.s. noise in each channel of the spectral line data was about 70 mJy beam^{-1} at the same angular resolution.

3. RESULTS

In Figure 1, we show the 1.4 mm continuum map and the integrated intensity $^{12}\text{CO}(2-1)$ line emission from HH

² The MIR-IDL cookbook by C. Qi can be found at <http://cfa-www.harvard.edu/~cqi/mircook.html>.

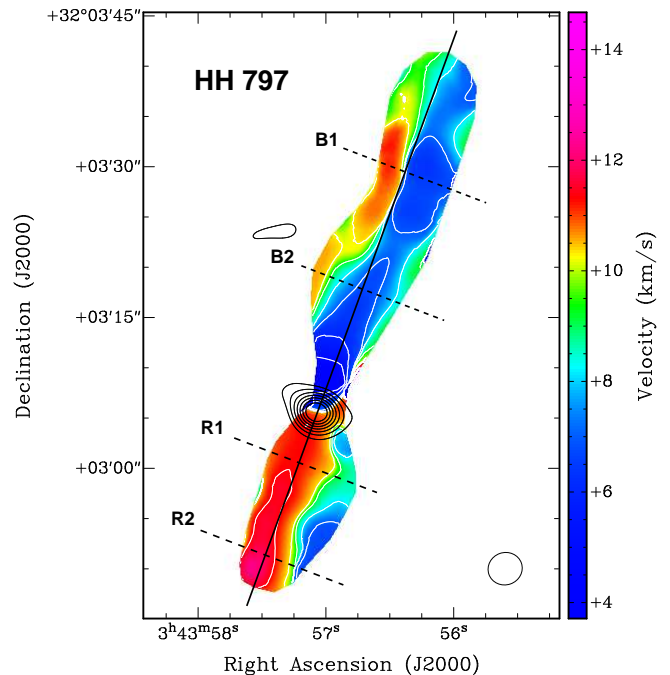


FIG. 2.— SMA CO(2-1) intensity-weighted velocity color map (moment 1) of HH 797 overlaid in contours with the 1.4 mm continuum emission (black contours) from the circumstellar disk associated with IC 348 MMS/SMM2, its exciting source. The black contours range from 30% to 90% of the peak emission, in steps of 10%. The emission peak for the millimeter continuum observations is $160 \text{ mJy beam}^{-1}$. The color-scale bars on the right indicate the LSR velocities in km s^{-1} . The E-W dashed lines mark the positions of the position-velocity cuts shown in Figure 3. The N-S continuous black line represents approximately the position of the outflow axis. The synthesized beam of the line and continuum observations is shown in the lower right corner.

797 overlaid on the Spitzer-IRAC $4.5 \mu\text{m}$ image. This IRAC band contains several H_2 transitions which trace shock-excited material (Smith & Rosen 2005) associated (in the present case) with the supersonic flow in HH 797. This image reveals the highly collimated outflow (with an opening angle of about 6° at a position angle of -30°) already mapped in CO lines by Tafalla et al. (2006) at a lower spatial resolution. From our observations, it is evident that the $^{12}\text{CO}(2-1)$ emission traces the innermost portion ($\sim 0.1 \text{ pc}$) of the outflow. The blueshifted radial velocities run from -2 to $+8 \text{ km s}^{-1}$ and the redshifted ones from $+10$ to $+20 \text{ km s}^{-1}$; the systemic LSR radial velocity of the ambient molecular cloud is at about $+9 \text{ km s}^{-1}$. These velocity ranges are in very good agreement with those reported by Tafalla et al. (2006). Most of the receding radial velocities (redshifted) of the outflow are located toward the south, while the approaching radial velocities (blueshifted) are toward the north. We note that the optical and infrared components of HH 797 have been extensively discussed by McCaughrean et al. (1994), Eislöffel et al. (2003), and Walawender et al. (2005, 2006).

The outflow emanates from IC 348-MMS/SMM2, a class 0 object (Eislöffel et al. 2003). Our observations resolve the dust emission from this source, with a deconvolved size of $(3.0'' \pm 0.3'') \times (1.5'' \pm 0.2'')$, at P.A. = $+50.0^\circ$. This implies a physical size of about $900 \times 450 \text{ AU}$ (assuming a distance of 300 pc) and an orien-

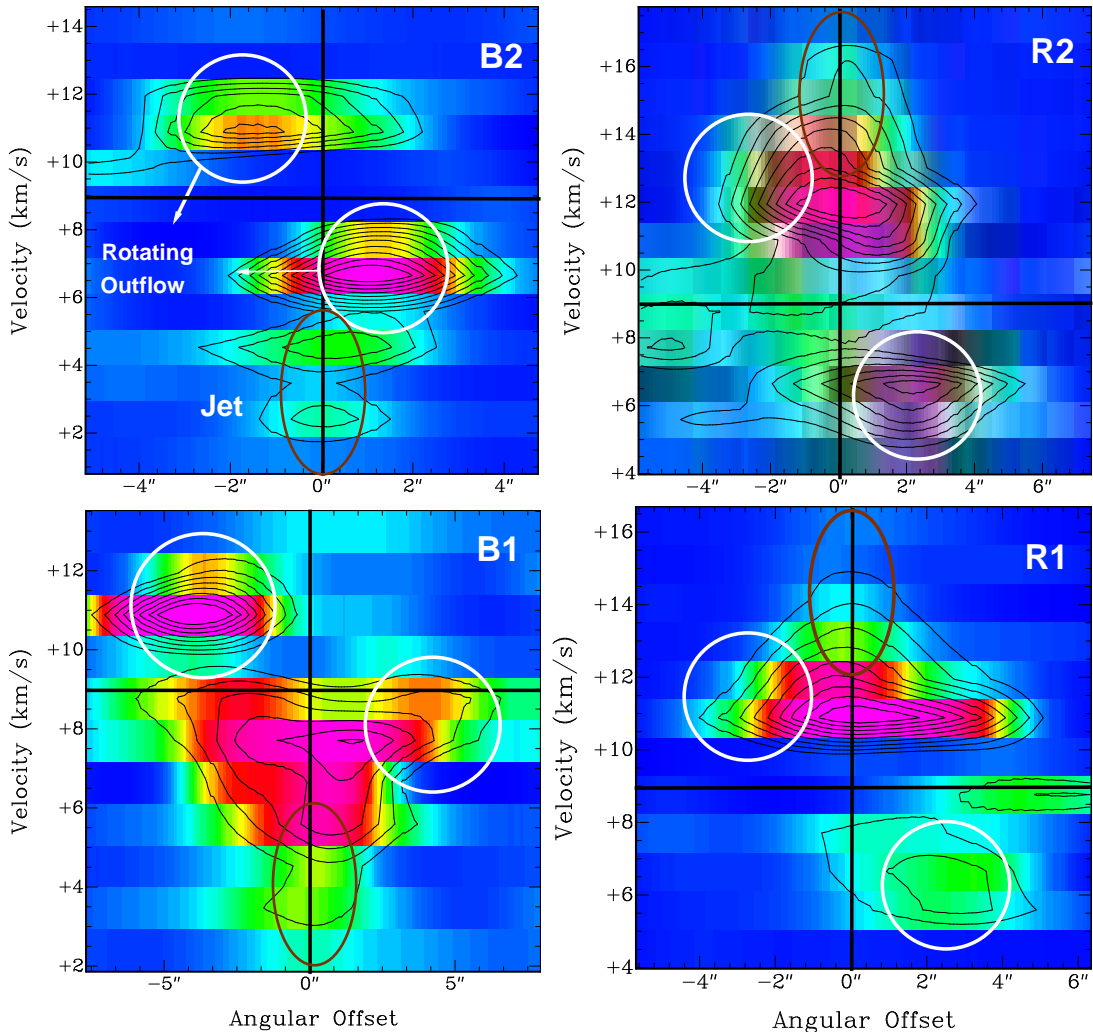


FIG. 3.— Position-velocity diagrams of the transversal cuts marked in Figure 2, across the outflow. The black contours range from 30% to 90% of the peak emission in steps of 10%. The black lines mark the position of the symmetry axis of the molecular jet and the systemic velocity of the cloud (about $+9 \text{ km s}^{-1}$). The velocity and spatial resolutions are approximately 1 km s^{-1} and $3''$, respectively. The spatial scale is in arcsec.

tation almost exactly perpendicular to the outflow axis. The source is centered at the $\alpha_{J2000.0} = 03^{\text{h}}43^{\text{m}}57^{\text{s}}.073$, $\delta_{J2000.0} = +32^{\circ}03'05''.59$ and has a flux density AT 1.4 mm of $220 \pm 15 \text{ mJy}$. Assuming optically thin isothermal dust emission, a gas-to-dust ratio of 100, a dust temperature of 40 K, a dust mass opacity $\kappa_{1.4\text{mm}} = 1 \text{ cm}^2 \text{ g}^{-1}$, and an emissivity index $\beta = 1.5$, we estimate a total mass for the source of $0.09 M_{\odot}$. This combination of properties suggest that the emission seen at 1.4 mm is dominated by the accretion disk, although a contribution from the inner envelope might also be present. In objects where the masses of the disks and central stars have been estimated, they usually are in a ratio of order $M_{\text{star}}/M_{\text{disk}} \sim 10$ (Rodríguez et al. 1998; Guilloteau & Dutrey 1998; Schreyer et al. 2006). This suggests that the central protostar in IC 348-MMS/SMM2 is roughly of solar mass. We searched for a centimeter counterpart using the Very Large Array archive data from project S9056, taken on 2008 March 13, 14, 18 and 19. We did not detect a source, setting $4\text{-}\sigma$ upper limits of 0.05 and 0.06 mJy at 4.86 and 8.46 GHz, respectively.

In Figure 2, we present the intensity-weighted velocity map of the $^{12}\text{CO}(2\text{-}1)$ emission, which confirms that most

of the redshifted velocities are found to the south, while the blueshifted velocities are to the north. Interestingly, this figure also shows a clear gradient *across* the outflow, detected along the entire length of the flow. This gradient is such that, at a given distance from the protostar, the velocity of the gas near the eastern edge of the jet is systematically more red-shifted than that of the gas on the western edge.

This asymmetry is confirmed by the position-velocity (PV) diagrams for four cuts across the outflow (Figure 3), which reveal the spatial structure of the gas across the flow as a function of the radial velocities. One can observe that in all cases, a "V"-shape (or, perhaps, more accurately, a triangular shape) velocity pattern is apparent. Near the axis of the jet, high and low velocities co-exist, extending from the systemic velocity up to about $+2 \text{ km s}^{-1}$ on the north (blue) side and about $+16 \text{ km s}^{-1}$ on the south (red) side. In contrast, near the edges of the flow, only comparatively low velocities are detected. If the velocity of the gas were parallel to the direction of the outflow, one would expect these V shapes to be symmetric with respect to the axis of the flow. In the

present case, however, there is a clear asymmetry. Consider, for instance, the cuts at positions B1 and B2. Near the western edge (at angular offset $\sim +5''$), the bulk gas is at a velocity of about $+8 \text{ km s}^{-1}$ (i.e. slightly below the systemic velocity, as appropriate for the blue side). But near the eastern edge (angular offset $\sim -5''$), the gas reaches redshifted velocity of about $+11 \text{ km s}^{-1}$. Similar patterns are seen at positions R1 and R2 and have been reported in two other collimated outflows (Orion-S6 and HH 212; Lee et al. 2008; Zapata et al. 2010) where they have been interpreted as evidence for outflow rotation. In the present case, the amplitude of the velocity asymmetry is about 2 km s^{-1} . We should mention, finally, that the structure of the emission at the systemic velocity (where the outflow emission is blended with the extended ambient emission) is poorly reconstructed by our interferometric data. The apparent lack of continuity in the PV diagrams at velocity $+9 \text{ km s}^{-1}$ is a result of this effect.

4. DISCUSSION

The most natural interpretation of the velocity asymmetries observed here is jet rotation. Let us, however, consider and discuss alternative explanations. The most obvious alternate interpretation would be that the flow driven by IC 348-MMS/SMM2 is in fact the superposition of two nearly parallel outflows, not spatially resolved by our observations, and powered by a central tight binary system. In a recent study, Murphy et al. (2008) present a model of such a situation, and show that the parallel outflows eventually merge, resulting in a persistent kink in the final structure. Moreover, the precession induced by the binarity quickly lead to bending jet trajectories. Although they cannot be entirely ruled out, neither of these effects are apparent in our SMA data. In addition, there is currently no independent direct evidence supporting the binarity of IC 348-MMS/SMM2.

A second possibility to consider is that of a precessing (non-rotating) jet/outflow system. This possibility would naturally fit with the "wavy" morphology of the outflow at large distances from the source, as revealed at infrared wavelengths (see Figure 1). This situation might plausibly mimic rotation because the jet would be the superposition of successive events where gas was ejected in different directions at different times. Such a scenario, however, does not easily explain the symmetric V-shape morphology seen in the PV diagrams of HH 797 (which are consistent, instead, with a high velocity jet along the outflow axis). In addition, precession should produce a point-symmetric situation: if the asymmetries were east to west along the blue outflow lobe, they should be west to east along the red lobe. In the present case, however, the asymmetry is consistently east to west along the entire length of the flow.

Since alternative interpretations fail to reproduce the observed kinematics of the HH 797 flow, we interpret the observed velocity asymmetries as rotation. Considering the situation where a jet is launched from a rotating

protostellar disk and then accelerated and collimated by MHD forces, Anderson et al. (2003) provide a formula relating the jet properties measured at large distances from the disk to the position (the "footpoint") on the disk where the jet is anchored.

$$\varpi_0 \approx 0.7 \text{ AU} \left(\frac{\varpi_\infty}{10 \text{ AU}} \right)^{2/3} \left(\frac{v_{\phi,\infty}}{10 \text{ km s}^{-1}} \right)^{2/3} \left(\frac{v_{p,\infty}}{100 \text{ km s}^{-1}} \right)^{-4/3} \left(\frac{M_*}{1 M_\odot} \right)^{1/3} \quad (1)$$

Here ϖ_∞ is the observed radial distance of the jet shell from the flow axis, ϖ_0 the radius on the disk from where that shell's material leaves, $v_{\phi,\infty}$ and $v_{p,\infty}$ are the toroidal and poloidal velocities observed for the shell at ϖ_∞ , and M_* the mass of the (proto)star at the center of the disk. In this case, we assume from observation $\varpi_\infty \sim 1000 \text{ AU}$ (about $4''$), $v_{\phi,\infty} \sim 2 \text{ km s}^{-1} \cos \alpha$, $v_{p,\infty} \sim 10/\sin \alpha \text{ km s}^{-1}$ and $M_* \sim 1 M_\odot$, with α the unknown angle between flow direction and plane of the sky. This results in a footpoint radius of $100 * (\sin \alpha)^{4/3} * (\cos \alpha)^{2/3} \text{ AU}$. Since the apparent poloidal flow velocity of $\sim 10 \text{ km s}^{-1}$ relative to ambient is relatively low, it seems likely that α is small. For $\alpha \leq 20^\circ$ the footpoint radius would drop to below 20 AU , a reasonable value that fits with the innermost part of the above-mentioned disk dimensions.

The value $\varpi_\infty = 20 \text{ AU}$ is very similar to the one found by Zapata et al. (2010) for the rotating outflow Ori-S6 energized by the young class 0 protostar 139-409 and the one estimated by Launhardt et al. (2009) for the the outflow CB 26 powered by a more evolved low-mass T-tauri star. On the other hand, Choi et al. (2011); Lee et al. (2009, 2008) have found much smaller values for ϖ_∞ in outflows powered for both class 0/1 protostars. Thus, at this point, we cannot rule out any conclusion about the variation of ϖ_∞ with time or some similarities on these values.

5. CONCLUSIONS

In this paper, we have reported $^{12}\text{CO}(2-1)$ line observation of HH 797, and discovered velocity asymmetries about the flow axis with an amplitude roughly on the order of 2 km s^{-1} over distances of about 1000 AU . The same velocity asymmetries are found on both sides of the outflow, and we interpret them as evidence for jet rotation. Thus, HH 797 appears to be promising laboratory for future studies of magneto-centrifugal models of jet acceleration.

G. P., L.A.Z., L. L. and L. F. R. acknowledge the financial support from DGAPA, UNAM, and CONACyT, México. L. L. is indebted to the Alexander von Humboldt Stiftung for financial support. We are grateful with the anonymous referee whose recommendations helped us to improve the paper.

Facilities: SMA, SPITZER (IRAC).

REFERENCES

- Anderson, J. M., Li, Z.-Y., Krasnopolsky, R., & Blandford, R. D. 2003, ApJ, 590, L107
 Choi, M., Kang, M., & Tatematsu, K. 2011, ApJ, 728, L34
 Eislöffel, J., Froebrich, D., Stanke, T., & McCaughrean, M. J. 2003, ApJ, 595, 259
 Gooch, R. 1996, Astronomical Data Analysis Software and Systems V, 101, 80

- Guilloteau, S., & Dutrey, A. 1998, *A&A*, 339, 467
- Hatchell, J., & Dunham, M. M. 2009, *A&A*, 502, 139
- Fendt, C. 2011, *ApJ*, 737, 43
- Ho, P. T. P., Moran, J. M., & Lo, K. Y. 2004, *ApJ*, 616, L1
- Launhardt, R., Pavlyuchenkov, Y., Gueth, F., et al. 2009, *A&A*, 494, 147
- Lee, C.-F., Ho, P. T. P., Bourke, T. L., et al. 2008, *ApJ*, 685, 1026
- Lee, C.-F., Hirano, N., Palau, A., et al. 2009, *ApJ*, 699, 1584
- Murphy, G. C., Lery, T., O'Sullivan, S., et al. 2008, *A&A*, 478, 453
- McCaughrean, M. J., Rayner, J. T., & Zinnecker, H. 1994, *ApJ*, 436, L189
- Pudritz, R. E., Ouyed, R., Fendt, C., & Brandenburg, A. 2007, *Protostars and Planets V*, 277
- Shang, H., Li, Z.-Y., & Hirano, N. 2007, *Protostars and Planets V*, 261
- Scoville, N. Z., Carlstrom, J. E., Chandler, C. J., et al. 1993, *PASP*, 105, 1482
- Smith, M. D., & Rosen, A. 2005, *MNRAS*, 357, 1370
- Schreyer, K., Semenov, D., Henning, T., & Forbrich, J. 2006, *ApJ*, 637, L129
- Tafalla, M., Kumar, M. S. N., & Bachiller, R. 2006, *A&A*, 456, 179
- Walawender, J., Bally, J., & Reipurth, B. 2005, *AJ*, 129, 2308
- Walawender, J., Bally, J., Kirk, H., et al. 2006, *AJ*, 132, 467
- Rodríguez, L. F., D'Alessio, P., Wilner, D. J., et al. 1998, *Nature*, 395, 355
- Zapata, L. A., Schmid-Burgk, J., Muders, D., et al. 2010, *A&A*, 510, A2